The International Journal of Advanced Manufacturing Technology (2022) 123:749–760
https://doi.org/10.1007/s00170-022-10157-8

ORIGINAL ARTICLE

Electrode wear investigation of aluminium spot welding by motion overlay

Stefan Heilmann[1] · Martin Baumgarten[1] · Johannes Koal[1] · Jörg Zschetzsche[1] · Uwe Füssel[1]

Received: 19 April 2022 / Accepted: 14 September 2022 / Published online: 30 September 2022

Abstract
The amount of aluminium sheets in future body-in-white concepts is still on the rise. There is a need for optimizing the joining techniques, caused by the different characteristics compared to the established steel components. Especially the electrode life for resistance spot welding as a reliable and established process needs to be improved. One reason for the short electrode life when welding aluminium is the insulating effect of the aluminium oxide layer. One possibility to reduce the electrode wear is the mechanical destruction of the oxide layer before the welding. This paper describes the influence of a translational and rotational electrode movement on the electrode wear. The oxide layer destruction is detected by resistance measurement. It could be shown that the destruction of the oxide layer already occurs at low movements. However, a homogeneous, large-area destruction is necessary for a wear reduction.

Keywords Aluminium alloys · Oxide layer · Resistance spot welding · Electrode wear

1 Introduction

Resistance spot welding is an established joining process for steel sheets in the automotive industry. Aluminium is used instead of steel to reduce the weight of the body. Aluminium alloys require higher electrode forces and welding currents. The major challenge is the high electrode wear as well as process stability compared to steel. Unknown contact resistances exist between the electrode and the aluminium sheet at each welding spot because of the natural, uneven oxide layer on the surface of aluminium alloys. Additionally, the electrical resistance of the oxide layer is higher than the one of the base material, with given values of $1 \times 10^{15}\Omega$ m and $6 \times 10^{-6}\Omega$ m respectively [1]. This influences the joule heating during the joining process. The high contact resistance causes higher amounts of heat. This leads to a steep rise in temperature. The chemical affinity between the copper electrode and the aluminium sheet is stronger than copper and zinc/steel [1, 2]. Both physical characteristics are responsible for the faster wear of the electrodes when welding aluminium than coated steel [1, 2]. Reducing contact resistance between electrode and sheet increase the electrode life time. This is essential to apply resistance spot welding for aluminium materials in a cost-effective way in car body construction.

Optimized electrode materials and geometries have been developed for welding aluminium alloys [1–4], to reduce the contact resistance. Kang et al. describe modification of the surface topography of electrodes in which ring-shaped structures in the sub millimetre range were milled into the electrodes [5]. These structures are up to 150 mm in depth and can break through the aluminium oxide layer during the welding process. As a result, less electrical contact between the electrode and the sheet can be achieved [6].

To stabilize the process welding electrodes are frequently dressed [1]. This method is economically disadvantageous due to the high welding downtime. Furthermore, the possibility is given to the usage of processing tapes, which are

✉ Stefan Heilmann
stefan.heilmann@tu-dresden.de

Martin Baumgarten
martin.baumgarten@tu-dresden.de

Johannes Koal
johannes.koal@tu-dresden.de

Jörg Zschetzsche
joerg.zschetzsche@tu-dresden.de

Uwe Füssel
uwe.fuessel@tu-dresden.de

[1] Technische Universität Dresden, Chair of Joining Technology and Assembly, Helmholtzstraße 5, Dresden 01309, Saxony, Germany

located between the electrodes and base material to avoid contamination [7]. The main problem is that the process tape cannot be reused and therefore the process costs are increasing.

The commonly known solutions for reducing the thickness of the oxide layer are chemical, physical or mechanical processes [1–3, 5, 8]. In chemical processes pickling is used with or without passivation [1]. In physical processes arc treatment can be used [1]. Other approaches are based on mechanical processes such as grinding or sandblasting that reduce the oxide layer [1–3, 8]. Neither process is performed directly before the welding process. For this reason, the oxide layer can form again. The processes only lead to a reduction, a complete avoidance of the oxide layer is not possible.

Taylor and Arrington developed a method to remove this layer mechanically [9], for reducing the regeneration time of the oxide layer. They proposed a relative movement around the electrode axis to destroy the layer. This movement as well as other possible motion overlays is shown in Fig. 1. The influences of the relative movement A and C on the electrode wear is investigated in this work. Suitable parameters for a translational as well as rotational movement around *y*-direction are shown and the cause of its effect is explained in more detail. The selection of the parameters used for the translational motion is based on the results of a previous publication [10]. In this publication an analogy experiment for the translation was performed. The results showed that long translation paths and high normal forces are leading to an accumulation of material in front of the electrode.

2 Materials and methods

The motion overlay experiments were carried out on a test rig shown in Fig. 2. The test rig is self-developed by the Technische Universität Dresden. Translations of the sheet in the *x*-direction and rotations of the electrodes around the *y*-direction are possible with the test rig. The motion directions correspond to the coordinate system shown in Fig. 1. A detailed description of the test rig can be found in [10]. The voltage between the electrodes is measured during the

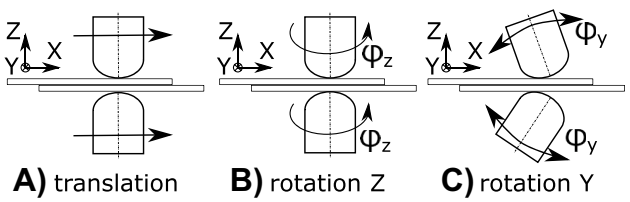

Fig. 1 Possible electrode movements to destroy the oxide layer on the sheets, **A** translation in *x*-direction, **B** rotation φ around *z*-direction, **C** rotation φ around *y*-direction

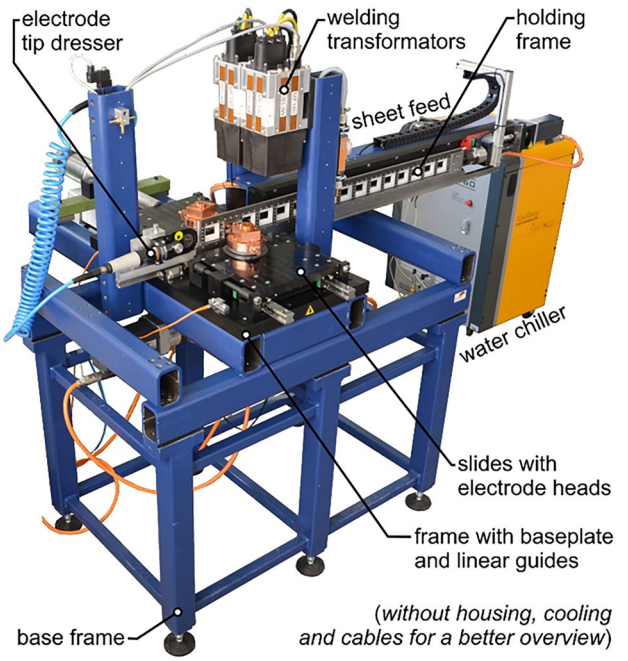

Fig. 2 Test rig for resistance spot welding with motion overlay by [10]

movement. For this purpose a precision current source delivers a measuring current.

The experiments were performed using two sheets of 50 mm length, 50 mm width and 2 mm thickness sheets of EN-AW-6016 (T4) as well as with the alloy EN-AW-5182. The chemical composition was measured by glow discharge spectroscopy and is shown in Table 1.

The welding and motion parameters are shown in Table 2. The force level of 350 N was omitted for the rotation because of problems with motion control.

Electrode caps according to ISO 5821-A0-16-22-150 made of CuCr1Zr were used. The influence of translation was investigated by three different sheet movements. In [10] it was shown that for small forces a long distance has a negative influence on the electrodes. For this reason, shorter distances were investigated at higher forces.

The length of the rolling path of the electrode around the *Y*-axis was determined according to the simulated contact radius of 2.9 mm in [4] at a welding force of 5 kN. The rolling path of 1 mm and 2 mm lies inside the contact radius. A rolling path with 3.5 mm lies outside the contact radius. The rotation

Table 1 Composition in wt-% for the used aluminium alloys

Alloy	Si	Fe	Mn	Mg	Al
EN-AW-5182	0,04	0,245	0,35	4,52	remainder
EN-AW-6016	1,14	0,3	0,08	0,41	remainder

Table 2 Parameters for experimental investigation of relative movement

Parameter	EN-AW-5182	EN-AW-6016
Welding Force in N	5000	5000
Welding Time in ms	60	60
Welding Current in kA	42	43.75
Amount of Welds	20	15
Force during Movement in N	350[a]; 500; 1000	350[a]; 500; 1000
Displacement in mm	1; 2; 3	1; 2; 3
Rolling Path in mm	±1; ±2; ±3.5	±1; ±2; ±3.5
Rotation Angle in °	±1; ±2; ±3.8	±1; ±2; ±3.8

[a]just translation

angles are calculated with the lever arm between the electrode-sheet contact surface to the axis of rotation and the radius of the crowning. The tests are named according to the scheme: motion overlay_force during movement_movement. The motion overlay can be "R" for rotation or "T" for Translation. For motion overlay "R" the movement is the rotation angle and for "T" the displacement shown in Table 2. T_1000_3 for example stands for the translation movement with 1000 N normal force and 3 mm displacement and R_1000_3.8 stands for the rotational movement with 1000 N normal force and 3.8° rotation angle. The process for translation with 3 mm sheet movement as well as the process sequence for an electrode rotation of ±3.8° at a force level of 1000 N is shown in Fig. 3. The movements are done within one second. The rotation must have only rolling friction, to understand the difference between translation and rotation. The sheets have to move over the same distance as the rolling path of the electrode, to achieve this.

The reference specimens were welded. For this purpose, the electrodes were evaluated after every five spot welds. The test was terminated, in the case of visible wear. Visible wear was defined as the tearing out of material from the electrode or alloying of aluminium on the electrode. The conducted welds until this point determine the service life of the electrode. 20 spot welds per test series were welded for the EN-AW-5182 alloy. 15 spot welds per test series were welded for the EN-AW-6016 alloy. 16 test series were carried out and evaluated per material, including the reference welding,.

The change in contact resistance during the movement is investigated as a criteria for the destruction of the oxide layer. The results were compared with the wear of the electrodes. To achieve a resilient comparison an objective evaluation of the wear is necessary. Therefore, electrodes were presented to 15 persons with experience in resistance spot welding. This allowed a subjective sorting by state of wear, from 1 to 16 in ascending order. This enables a statistical analysis of the subjective wear evaluation. The maximum torque of failure was determined in the torsion test according to EN ISO 17653 [11]. Based on the destructively tested specimens the weld diameter was measured.

3 Results

The wear evaluation is shown in Fig. 4a and b as the median with upper and lower quartiles as well as the upper and lower whiskers. The outliers are defined by values more than 1.5 x difference of the length of both quantiles.

The subjective assessment of wear varies. The anodes for every welding test are shown in Figs. 13 and 14. As an example the comparison of the anode for test R_1000_2 and R_1000_3.8 for alloy EN-AW-5182 in Fig. 14 can be viewed. For the 2° rotation the opinions varied in the wear raking from 1 to 8 with a median at 2, where 8 is an outlier. The 3.8° rotation was rated from 4 to 16 with a median of 12. This indicates that the wear conditions can not be evaluated clearly by an optical evaluation.

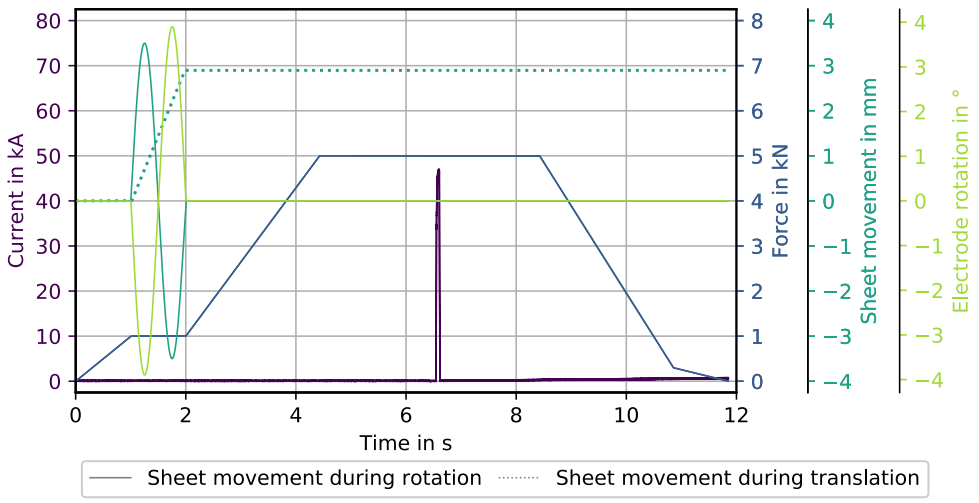

Fig. 3 Example of the process for sheet movement during translation (T_1000_3) and during rotation (R_1000_3.8), for same current and force

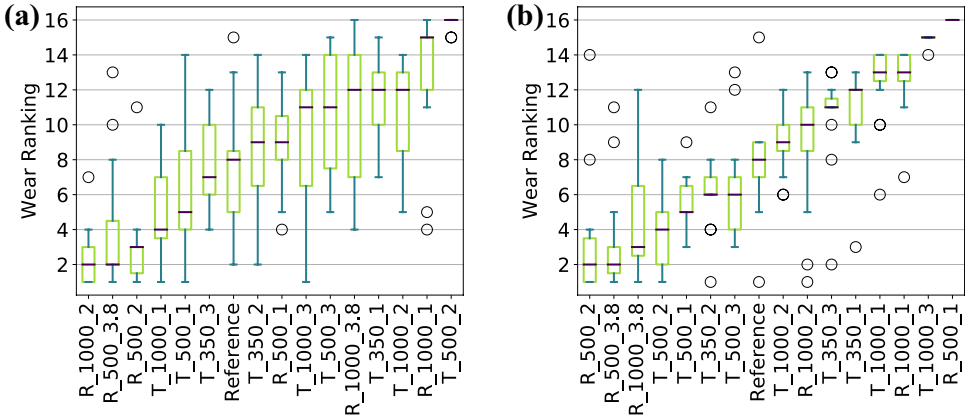

Fig. 4 Ranking of the wear assessment of the electrodes with different motion overlays, arranged according to the subjective wear evaluation of 16 people for **a** EN-AW-5182 and **b** EN-AW-6016, the smaller the number, the better; visualization as boxplot; Designation of the sample names in the x-axis according to the scheme: motion overlay_force during movement_movement

The differences in the evaluation between both alloys can be seen by the minimal and maximal values as well as the quantiles of both figures. Both alloys showing nearly the same differences in the minimal and maximal values. For the alloy EN-AW-5182 the quantiles are larger than for the alloy EN-AW-6016. The most minimal and maximal values for the EN-AW-6016 alloy are outliers. That is due to the closer quantiles. This indicates, that the evaluation of the EN-AW-6016 is more clearly. For a wear evaluation of rating 16 no quartiles are present and thus this rating is clear. No absolute statement about the best motion overlay can be given, due to the partially similar wear ranking for the different movements. Nevertheless, the following can be concluded for wear improvement. A short movement is necessary, for translation. The angle of rotation and respectively the resulting rolling path must be as large as possible, for the rotation. The forces have not a significant role. Only the results of the alloy EN-AW-6016 will be discussed further below, since the order of the wear ranking for both alloys is about the same.

A constant measuring current of 50 A was used to measure the voltage between the electrodes. The total resistance was calculated. The change in resistance during the movement was used as a measure of the effect of movement on the oxide layer. Figure 5 shows the average values for the 15 spot welds before the start of the movement and at the end of movement. The tests are arranged on the *x*-axis according to the wear ranking in Fig. 4b.

Before the start of the movement the resistance is irregularly distributed. Furthermore, a strong deviation of the values is evident. These phenomena are caused by the uneven oxide layer as well as the electrode wear. No systematic increase during the tests is visible, Regarding the influence of the wear on the resistance in the data. The resistance before the movement decreases with higher forces, as does the deviation. A higher force leads to levelling of the roughness and therefore a larger contact area. The resistance as well as its deviation is reduced due to the movement. This can be attributed to the destruction of the oxide layer.

The spot diameter as well as the electrode wear depends strongly on the resistance at the applied welding force. The resistance with applied welding force is shown in Fig. 6 in comparison to the resistance after the motion overlay.

There is a further decrease in resistance as well as a decrease in deviation in all tests, with higher electrode force. This is an expected behaviour, since it is generally

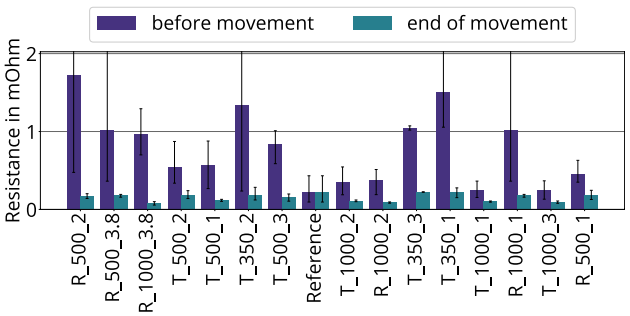

Fig. 5 Resistance before and at the end of electrode movement, in order of the electrode wear ranking for EN-AW-6016

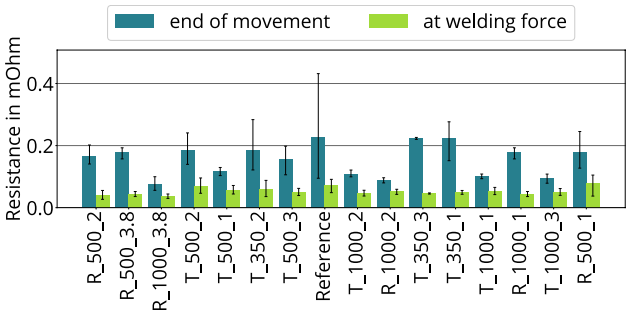

Fig. 6 Resistance at the end of electrode movement and at welding force of 5000 N, in order of the electrode wear ranking for EN-AW-6016

known that resistance decreases with increasing force. A higher force results in a stronger levelling of the roughness peaks and an increase in surface area. Furthermore, a difference between the rotation and the translation can be seen. A lower resistance leads to a lower wear in the case of rotation. The translation shows an opposite behaviour. The reference test, which is evaluated as neutral wear, shows the highest resistance before the start of welding.

For a better explanation of the process the progression of the resistance for translation is shown in Fig. 7a. The course of motion is depicted by the black curve. The diagram shows the average value of the resistance for the respective series of experiments. The resistance drops the largest amount right at the beginning of the movement in all experiments. This also represents the lowest resistance in most experiments. A recurring increase and decrease of the resistance can be observed during the translational movement for small forces of 350 N. This is most obvious for the translation of 1 mm. Also evident is an increase in resistance during the motion after the first drop. This is also found in the tests with 500 N. This behaviour is not apparent for forces of 1000 N. The resistance decreases continuously during the movement. However, an influence between the resistance curve and the wear rating in Fig. 4a and b is not evident.

Analogously to the translation, Fig. 7b shows the resistance over the rotation. Here, the resistance drops directly at the beginning of the movement. The resistance is lowest at the end of the movement in contrast to the translation. Resistance peaks can be seen at several points of the movement during the movement. For the rotation of 1° and 2°, these peaks occur only at the initial position of the electrode. A steady resistance drop occurs during the movement at the beginning of the rotation. After 0.5 s at the first zero crossing is an increase in resistance. The increased resistance is no longer reduced until the end of the movement for the rotation of 1°. A further reduction of the resistance is evident for the rotation of 2°. The height of the resistance peaks increases with increasing rotation angle. The resistance peaks can be explained by the change in normal force shown in Fig. 8.

During the tests, it became apparent that a rotation with only rolling friction is not possible under the given conditions. This is due to the construction of the test rig. The cap miller has no path compensation. The electrode dressing process is asymmetrical, if the caps do not touch exactly in the zero plane of the cap miller. This leads to an oblique crowning. Therefore, the movement curves of the electrodes calculated for force control do not work. As a result, the force exceeds or does not reach the calculated curve. This is shown in Fig. 8. The larger the rotation angle, the less time does the control have to readjust the force, which means that the force is greater at this point. Especially at the turning point of the electrodes, the difference between theoretical and real crowning is the largest. For this reason, the force changes sharply due to the asymmetrical caps. This also causes a force-dependent change in resistance. This makes it difficult to evaluate the influence of rotation on resistance. It can be seen that most of the change in resistance is due to the change in force. From these results the assumption can be made, that it could be an almost constant resistance when rotating the electrode.

The results of the torsion test are shown in Fig. 9 for both alloys to evaluate the influence of the electrode movement on the welding. The plot shows the maximum torque as well as the weld diameter including the deviation.

Based on the results, no clear statement can be made on the influence of the motion overlay. The torque and weld diameter are in the range of the reference. During the measurement of the weld diameter, deviations were found between the two measurement directions. For this reason, the ratio of both directions is shown in Fig. 10. The diameter d1 is measured in the direction of motion and d2 perpendicular to the direction.

For the translational motion overlay with forces lower than 1000 N, a ratio of one or greater was determined in

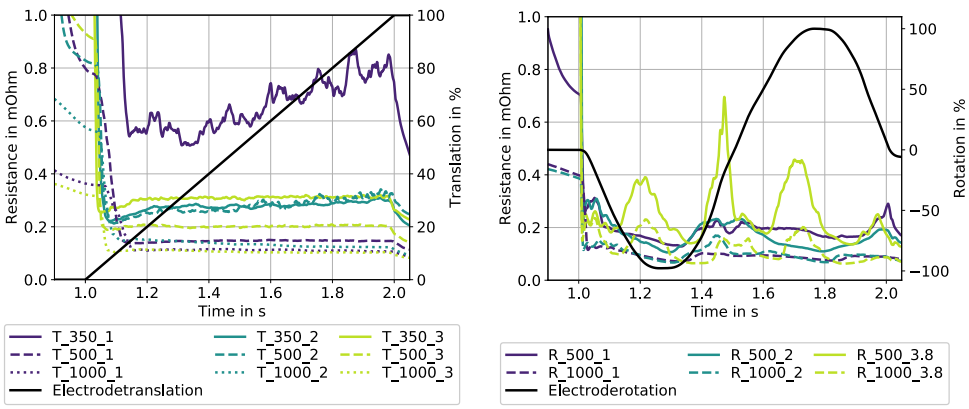

(a) Translation **(b)** Rotation

Fig. 7 Average resistance curves for the alloy EN-AW-6016 during **a** translational movement and **b** rotational movement

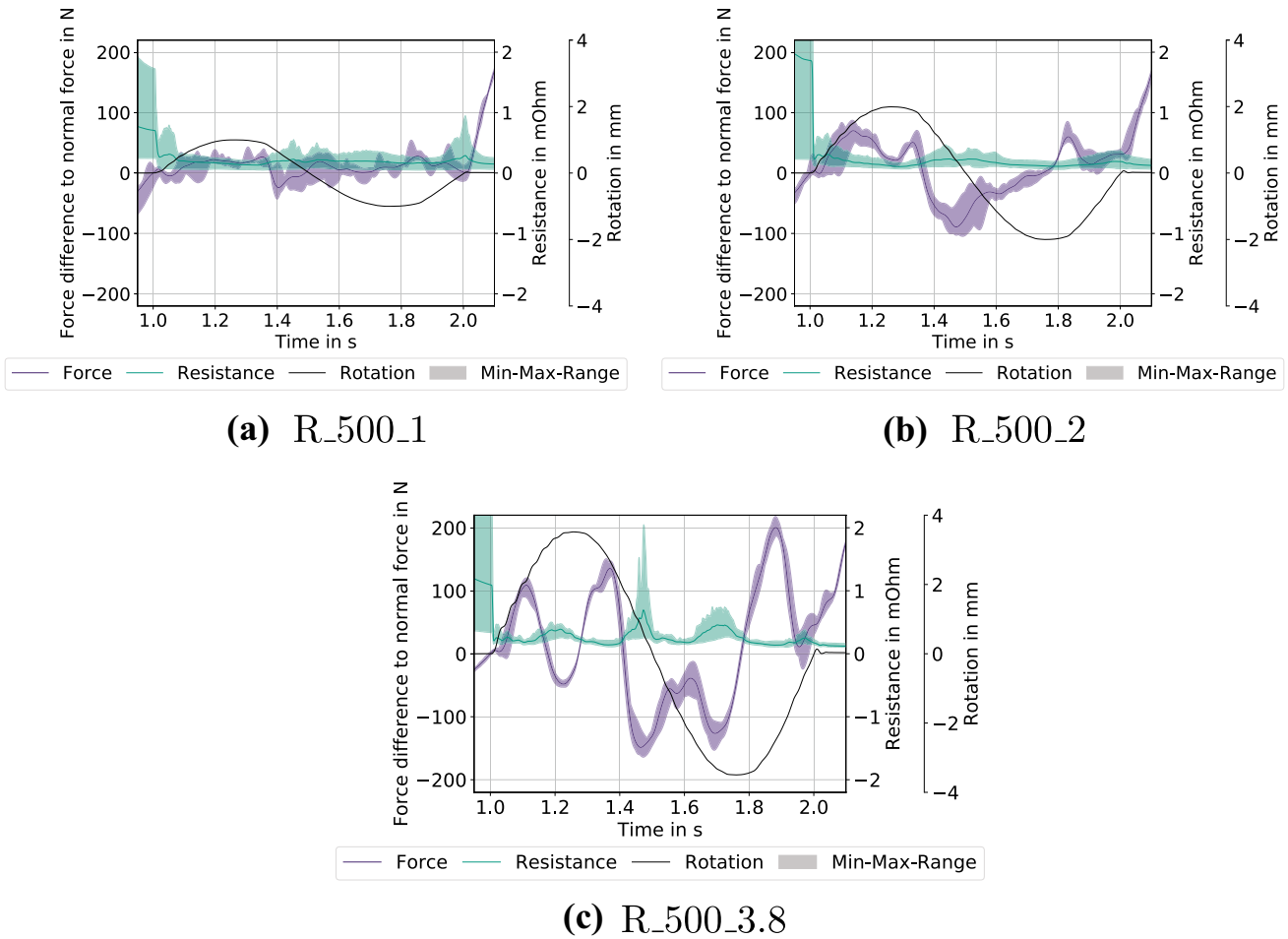

Fig. 8 Curve of mean resistance and mean normal force with min and max range for 16 measurements during rotational movement of **a** 1°, **b** 2° and **c** 3.8° with a force of 500 N of EN-AW-6016, angle converted to rolling path in mm

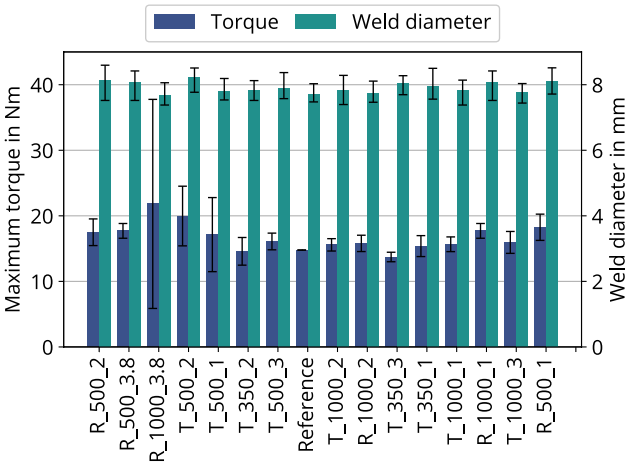

Fig. 9 Maximum torque at joint failure and mean weld diameter with deviation, in order of the electrode wear ranking for EN-AW-6016

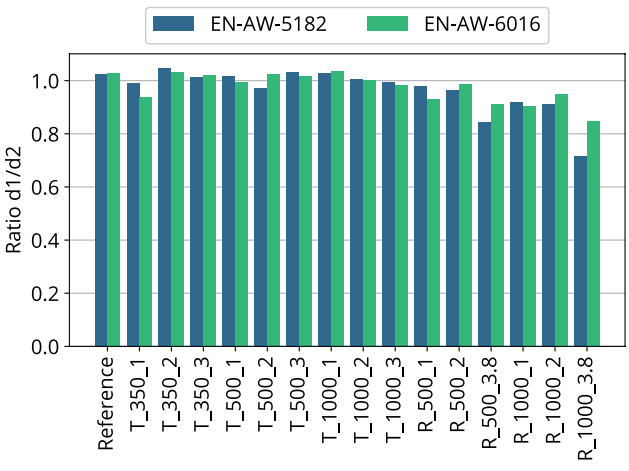

Fig. 10 Ratio of weld diameters d1 (in the direction of motion) and d2 (perpendicular to the direction of motion) for alloys EN-AW-5182 and EN-AW-6016

most cases. This corresponds to a larger expansion of the spot weld in the translation direction, and thus corresponds to the characteristics of the reference test. The translational motion with a force of 1000 N and the rotational motion, the spot grows in the direction of d2. The expansion in this direction increases with greater force and greater rotation angle. This behaviour is evident for both alloys.

4 Discussion

4.1 The influence of the contact resistance

The improvement of the electrode wear is often explained by reducing or breaking of the oxide layer. This leads to a lower contact resistance, which results in less local overheating [8, 12, 13]. In Fig. 5, a reduction in resistance for all motion overlays is shown. This is an indication of increased metallic contacts. The differences in resistance between the types of motion are reduced by the subsequent increase of forces up to 5 kN for welding, with the resistance of the reference weld being the largest (compare Fig. 6). The force-dependent changes can be attributed to the levelling of the roughness as well as the increase in contact area. This further breaks down the oxide layers as well as increases the effective area with metallic contacts. If the electrode wear would only depend on the resistance before welding, the results in Fig. 6 would mean that any motion overlay leads to a reduction in wear. That this is not the case is shown in Fig. 4a and b. The reference welding is in the middle of the wear evaluation.

Therefore, an average value over the entire time of the motions cannot be used exclusively as a statement about the electrode wear. That the resistance curves are much more complex can be seen in Fig. 7a and b. The curves show that for both motions the resistance drop occurs directly at the beginning of the motion. These results correlate with the results on translation shown in [10]. Crinon and Evans [8] also demonstrated this behaviour for rotation about the electrode axis. By converting the motion over time shown in Fig. 7a and b into the actual displacement, the resistance drop occurs within the first 0.15 mm. Following the drop, different resistance curves occur, depending on the motion. In the end, these influence the electrode wear due to local changes of the contact. A homogeneous resistance and thus current density distribution can be assumed [4] in the reference test. Local mechanical stress increases when moving the electrode. This leads to mechanical electrode wear due to the wear mechanisms adhesion, abrasion, surface disruption and tribochemical reaction [14]. Thus, thermal electrode wear, caused by alloying or cratering, is also significantly dependent on mechanical electrode wear. These two electrode wear mechanisms are locally different. Therefore, both will influence the local resistance and current density distribution in the contact area differently. With the conducted measurement, only the influences on the integral resistance over the entire contact area can be determined. Therefore only hypothesis can be found about these local changes.

4.2 The tribological system

A tribological system with different friction and wear types is established during the mechanical electrode wear process in both motion overlays. The electrode is the counter body and the sheet metal the base body. The rotation around the *y*-axis corresponds to the rolling friction while the translation causes sliding friction. This means that the electrode is stressed over a large area and always forms a new contact point with the sheet metal. The predominant friction mechanism is plastic deformation, which leads to surface disruption. The contact point on the electrode to the sheet metal remains the same during translation. Thus, always the same area of the electrode is stressed. A primarily furrow with possible adhesion as shown in [10] in the case of sliding friction, especially with aluminium alloys. The high plasticity as well as the low modulus of elasticity of sheet and electrode favours this adhesion [14]. Oxide particles will be formed and abrasive phenomena additionally occur [14] during the translation. Higher mechanical electrode wear is expected for translation than for rotation due to the characteristics of the two motions. This is supported by the electrode wear evaluations in Fig. 4a and b.

Both processes are subjected to nearly equal boundary friction, assuming an equal oxide layer as well as surface oiling at the start of motion. Therefore, it can be assumed approximately, that also the same processes take place on the micro level at the beginning. This explains the same drop in resistance at the beginning of the two movements (cf. Fig. 7a and b). A frictional force acts on the contact surface in addition to the normal force due to the movement. This leads to shear and compressive stresses, which cause the destruction of the oxide layer. The type of wear shifts toward solid-state wear [14] when the boundary friction is exceeded for the translation. The theoretically developed wear volume W_v can be calculated for sliding friction via Archard's law with Eq. 1 [14]. The equation describes the correlation of the wear coefficient k, the normal force F_N and the sliding distance s with the wear volume.

$$k = \frac{W_v}{F_N s} \tag{1}$$

4.3 Translational movement

From the Eq. 1, it can also be seen that the wear volume W_v increases with increasing normal force and increasing sliding distance. For translation, this results in an ever growing

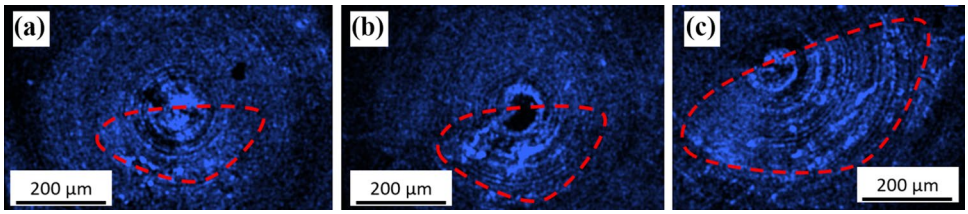

Fig. 11 EDX analysis of Al accumulation in front of the electrode (red dotted line) with magnification of 15x for **a** T_500_1, **b** T_500_2, **c** T_500_3

accumulation of material with longer movement and increasing force. In tests with translational movements on a scratch tester, it was found that material accumulation (adhesion and chip formation due to abrasion) and over-slip of these occurs, resulting in variations of resistance [10]. This recurring increase and decrease in resistance were only detected in one test series (T_350_1) (compare Fig. 7a). As described above, a strong deviation of the resistance curves between the individual welding tests occurred. This can be seen especially for this combination of motion. A possible cause could be the asymmetric dressed electrodes. An increase and decrease of the resistance could not be detected in the tests with longer translational movement. That the test series (T_350_1) is an exception can be assumed from this result. Thus, the results from [10] cannot be confirmed completely.

One reason for the difference to [10] can be found in the electrodes used. In this work electrodes with a crowning of 150 mm were used, while in [10] a crowning of 8 mm and 10 mm was used. This changes the angle of contacting surfaces between the electrode and the sheet and thus influences the abrasion. The steeper the angle, the more material is removed [14]. This means that greater chip formation occurred in [10], leading to the large material accumulations detected. Furthermore, the larger contact area for caps with a crown of 150 mm results in a low surface pressure. This reduces the penetration of the electrode into the sheet and will lower the amount of material in front of the electrode as well as the abrasive and adhesive behaviour at the electrode. In addition, the distance moved is much less. For these reasons, a different electrode wear behaviour and thus a different progression of contact resistances is the result.

Due to the interaction of the four mechanical wear mechanisms. The thermal electrode wear effects of alloying can be removed, or cratering can be increased. A prediction about the effect of movement on thermal electrode wear is difficult. An increasing resistance curve can always be seen during the movement for forces up to 500 N (compare Fig. 7a). This indicates a continuous accumulation of material in front of the cap or adhesion to the cap. These accumulations are shown in Fig. 11. With longer translation movement, the accumulation area, where more Al can be found, is growing.

In theory, this leads to higher mechanical and thermal electrode wear. However, at these low surface pressures, translational motion does not appear to reproducibility

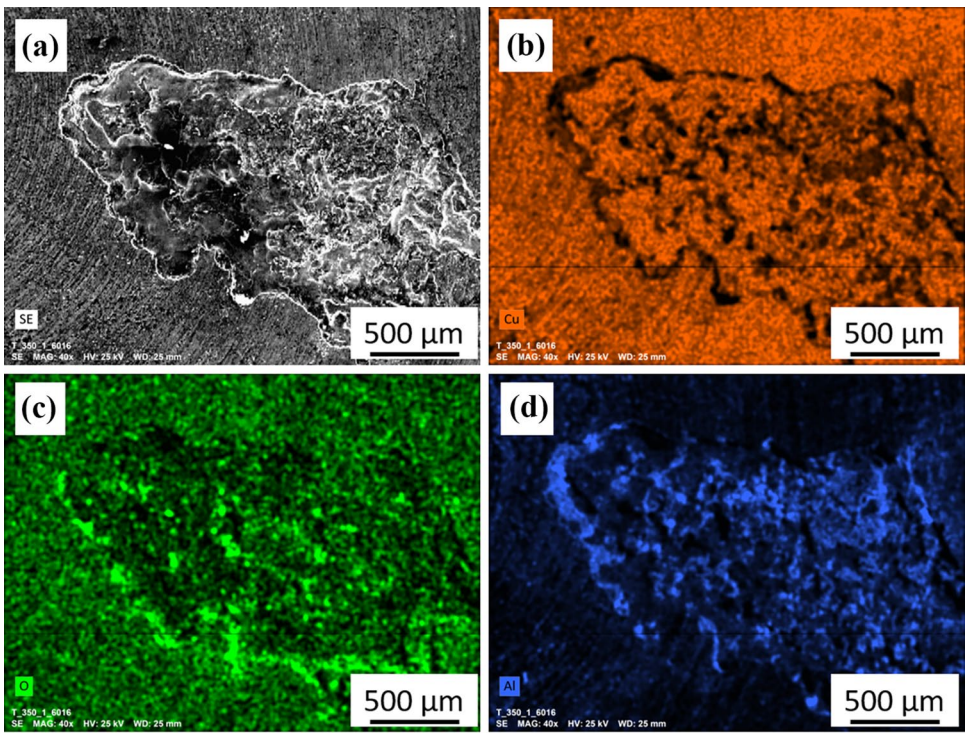

Fig. 12 SEM and EDX analysis of e crater from the electrode surface of T_350_1 with magnification of 40x; **a** SE picture, **b** Cu distribution, **c** O distribution, **d** Al distribution

influence thermal electrode wear. The influence of alloying, abrasion and material accumulation depends much more on the irregular aluminium surface. Depending on the surface, sometimes a long and sometimes a short path can be advantageous in combination with low surface pressure. Additional tests have to be carried out to determine the optimum path length in which each surface is examined in advance regarding the oxide layer thickness as well as roughness.

The higher the surface pressure, the shorter the path can be in order to obtain a positive influence on the electrode wear (compare Fig. 4). This can be explained by improved chip formation. The electrode penetrates deeper into the material, the oxide layer is destroyed and the contact surface no longer slides over the surface roughness at the beginning of the movement. Thus, with longer movement, more and more material is accumulated in front of the electrode. The longer the movement, the more metallic contacts will exist, causing the resistance to drop further. The thesis is confirmed by the decreasing voltage curve at normal forces of 1000 N (see Fig. 7a). Since no rising in the resistance curve can be detected, no sliding over the material accumulations will be present. This means the material has to accumulate in front of the electrode. The described increasing metallic contact between electrode and sheet should lead to an improvement of the thermal effected electrode wear. However, the electrode wear evaluation (Fig. 4a and b) showed greater electrode wear for a higher force. This can be attributed to the accumulation of material that formed in front of the electrode. Increasing the force to 5 kN after the movement also increases the contact area. Thus, the material accumulations formed are included in the area of the current conducting surface on one side. Due to the accumulated oxide particles, these material accumulations have a very high resistance. This leads to a strongly inhomogeneous current density distribution and thus to an uneven temperature distribution. This leads to a locally temperature increase, which favours wear in these regions. This thesis can also be confirmed based on the ratio of the weld diameters of the different directions in Fig. 10. The longer the sliding distance at high force, the smaller the ratio $\frac{d_1}{d_2}$ becomes. The accumulation in the contact plane leads to a higher contact resistance and thus to a reduction of the current density in the direction of motion. The heating and thus the expansion of the weld is shifted perpendicular to the direction of motion. For the 350 N and 500 N forces, no tendency is evident as the displacement increases. This correlates with the previously described non-uniform electrode wear mechanisms. As thermal electrode wear progresses, mechanical electrode wear will also have an increasing impact. Translational movement can remove alloying, but also enlarge resulting craters in the electrode. It is also possible for oxide particles to become trapped in the craters. This is shown in Fig. 12.

The EDX analysis shows mainly copper in the crater. At the different levels of the eruptions Al and also oxides are measurable. Especially in the edge area oxides are more measurable. The described processes result in increased local resistance which leads to an inhomogeneous current density and therefore causes a local temperature increase. This again increases thermal electrode wear. Based on the existing integral resistance measurements and the optical 2D documentation of the electrode wear, these phenomena cannot be described unambiguously. In further investigations, these theses have to be confirmed.

4.4 Rotational movement

As can be seen from Fig. 7a and b, the rotational motion has a better electrode wear rating than that of the translational motion. In addition, large angles and forces are beneficial in rotation. This can be attributed to the bigger area of the stressed region of the surface. In translational motion, the amount of destroyed oxide layer in the contact hardly changes. In the case of rotation, the stressed surface, in which the resistance was reduced, increases with increasing force and rotation distance. This leads to an overall larger area with better current density distribution. Therefore, the thermal wear is better for the motion with higher angles.

The rotational motion should mainly show surface disruption due to the rolling wear. As shown in Fig. 13, from, e.g., Anode R_500_3.8, also sliding friction occurs. This results in furrow formation, because of the changes in force during motion, evident in Fig. 8. This indicates a system that does not roll smoothly and therefore no friction free rolling was achieved. Thus, more complex processes, than only surface disruption, occur in the contact area. Due to the force peaks, the surface is deformed more compared to lower forces, which leads to a lower resistance in this area. More material would accumulate in front of the electrode, if a simultaneous sliding friction occurs. The oxide layer will be deformed less, if the force is reduced. With simultaneous sliding friction, the electrode could slide over the oxide layer without breaking it up. However, the resulting forces behind the electrode could lead to a breakup and thus favour the deposition behind the electrode. This leads to an increase in resistance in this area. In addition, particles generated by abrasion will adhere to the electrode and influence the further behaviour towards surface disintegration. The effects increase with larger rotation angles and higher contact forces. This leads to large force changes, especially in the turning points. Thus, analogous to translation, resistance maxima arise on both sides, which leads to a change in current density. This thesis can be confirmed with Fig. 10. The diameter d2 increases significantly with larger force and rotational displacement because of the higher contact resistance in the d1 direction.

Further testing and simulations are needed to better understand the influence of rotational motion.

5 Conclusions

In this paper it was shown, that a motion overlay before the welding can reduce the electrode wear. This is due to mechanical induced stress at the contact area. Therefore, the oxide layer is destroyed, which influences the thermal electrode wear. Movements exceeding a path length of 0.15 mm will destroy the oxide layer. Regardless of translation or rotation. It can be deduced that an effective reduction in electrode wear depends on the area, where the oxide layer is destroyed. It is important to break the entire contact area relevant to welding. This will achieve a more homogeneous current density in the contact interface. Therefore, uniform and lower thermal electrode wear will appear, which extends the electrode life. The main problem when describing the influence of the electrode movement is the highly subjective description of the electrode wear. In addition a longer electrode movement leads to complex mechanical electrode wear phenomena, which are difficult to map. Because of these two aspects only theses regarding the reasons of reduced wear could be formulated. Further investigations must be carried out to examine the described phenomena in more detail.

Appendix

Pictures of anodes

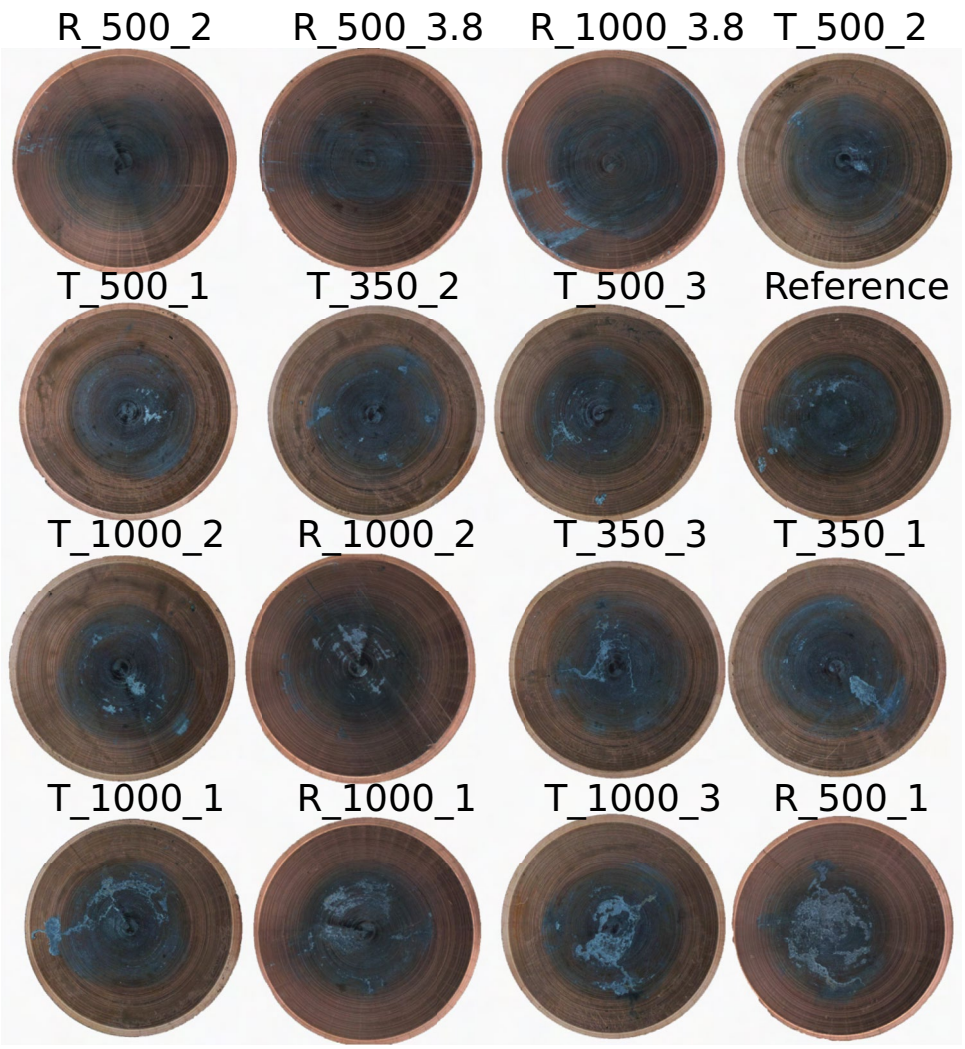

Fig. 13 Anodes after 15 spot welds for the alloy EN-AW-6016 sorted by wear ranking

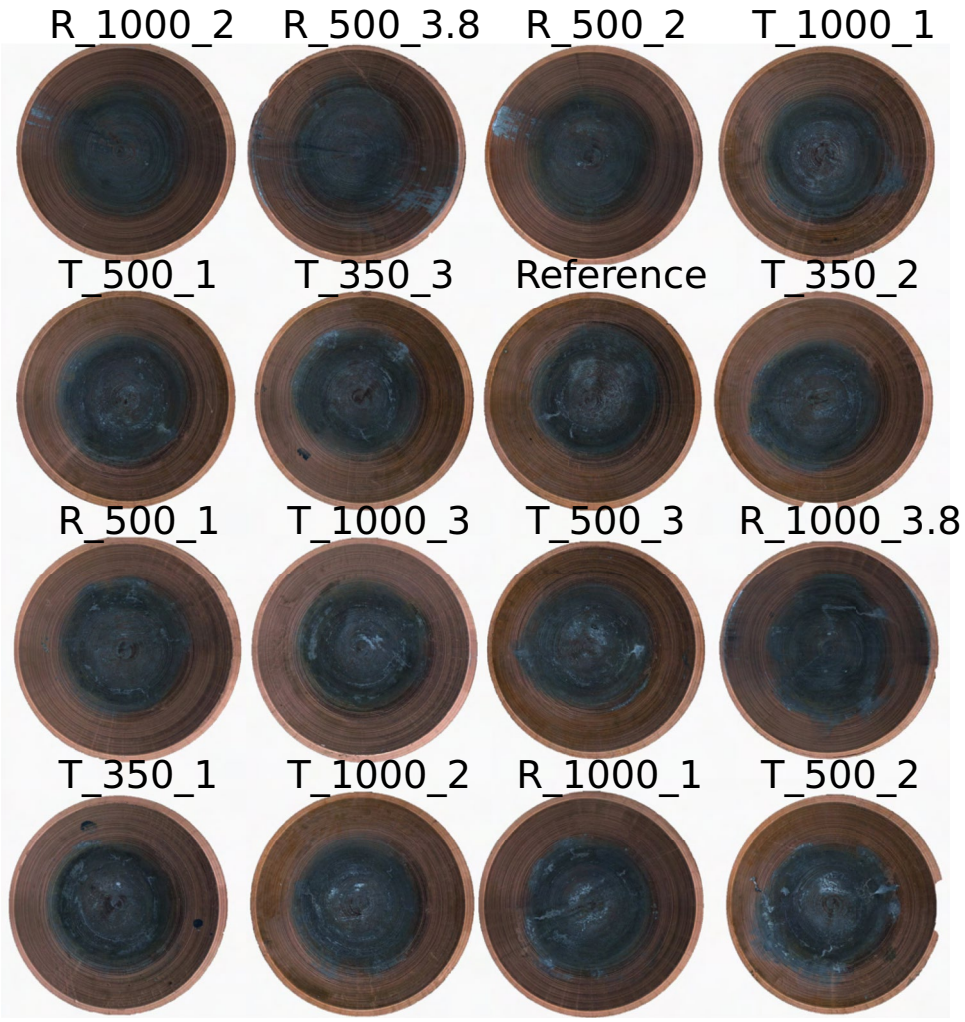

Fig. 14 Anodes after 20 spot welds for the alloy EN-AW-5182 sorted by wear ranking

Author Contributions Conceptualization, S.H.; methodology, S.H.; software, S.H.; validation, S.H.; formal analysis, S.H.; investigation, S.H.; resources, S.H.; data curation, S.H.; writing—original draft preparation, S.H.; writing—review and editing, S.H., M.B., J.K.; visualization, S.H.; supervision, U.F.; project administration, J.Z.; funding acquisition; U.F., J.Z. All authors have read and agreed to the published version of the manuscript.

Funding Open Access funding enabled and organized by Projekt DEAL. This research was funded by the Deutsche Forschungsgemeinschaft (DFG, German Research Foundation) within the project "Simulation-based analysis of resistance welding processes with motion overlay" under grant numbers FU307/11-1 resp. IH124/9-1, project no.: 266896522. Open Access Funding by the Saxon State and University Library Dresden (SLUB).

Availability of data and materials Data can be requested from the corresponding author.

Declarations

Ethics approval This paper is new. Neither the entire paper nor any part of its content has been published or has been accepted elsewhere. It is not being submitted to any other journal as well.

Conflict of interest The authors declare no competing interests.

References

1. Rashid M (2017) Some influences of tribology in resistance spot welding of aluminum alloys. Dissertation, University of Waterloo
2. Chan KR, Scotchmer NS (2022) Quality and electrode life improvements to automotive resistance welding of aluminum sheet. http://

huysindustries.com/wp-content/uploads/huysarticle17-Quality_and_Electrode_Life_Improvements_to_Automotive_Resistance_Welding_of_Aluminum_Sheet.pdf. Accessed 02 Aug 2022
3. Edwards PC, Flewelling E (2016) Aluminium resisatance spot welding tip and method of making the same. US 2016/0039039A1
4. Tuchtfeld M, Heilmann S, Füssel U et al (2019) Comparing the effect of electrode geometry on resistance spot welding of aluminum alloys between experimental results and numerical simulation. Welding in the World. https://doi.org/10.1007/s40194-018-00683-z
5. Kang J, Chen Y, Sigler D et al (2015) Fatigue behavior of dissimilar aluminum alloy spot welds. Procedia Eng 114:149–156. https://doi.org/10.1016/j.proeng.2015.08.053
6. Sigler DR, Carlson BE, Janiak P (2013) A recently developed electrode design features multiple protruding rings that penetrate oxide layers by straining the aluminum sheet surface during welding. Welding Journal June:64–72
7. Becirovic A (2010) Advantages of DeltaSpot when welding aluminium alloys and the experiences with SORPAS simulation. The 6th International Seminar on: Advances in Resistance Welding
8. Crinon E, Evans JT (1998) The effect of surface roughness, oxide film thickness and interfacial sliding on the electrical contact resistance of aluminium. Materials Science and Engineering: A 242(1–2):121–128. https://doi.org/10.1016/S0921-5093(97)00508-X
9. Taylor GA, Arrington SE (1994) Method and apparatus for spot welding. US005541382
10. Heilmann S, Köberlin D, Merx M et al (2019) Numerical and experimental analysis on the influence of surface layer on the resistance spot welding process for the aluminum alloys 5182 and 6016. Welding in the World 114(3):1700755. https://doi.org/10.1007/s40194-019-00743-y
11. European Commitee for Standardization (2012) Resistance welding - Destructive tests on welds in metallic materials - Torsion test of resistance spot welds (EN ISO 17653)
12. Patil RR, Anurag Tilak CJK, Srivastava V et al (2013) Minimising electrode wear in resistance spot welding of aluminium alloys. Science and Technology of Welding and Joining 16(6):509–513. https://doi.org/10.1179/1362171811Y.0000000036
13. Zhang WJ, Cross I, Feldman P et al (2016) Electrode life of aluminium resistance spot welding in automotive applications: a survey. Sci Technol Weld Join 22(1):22–40. https://doi.org/10.1080/13621718.2016.1180844
14. Wen S, Huang P (2018) Principles of tribology, 2nd edn. Wiley, Hoboken, NJ. https://doi.org/10.1002/9781119214908